AIMS Mathematics, 10(12): 28243–28263.
DOI: 10.3934/math.20251242
Received: 30 September 2025
Revised: 18 November 2025
Accepted: 21 November 2025
Published: 01 December 2025

https://www.aimspress.com/journal/Math

*Research article*

# Hopf bifurcation of uncertain nonlinear differential equations

**Xiuying Guo[1], Caiyun Huang[1], Qiubao Wang[1,2,*], Zikun Han[2], Zeman Wang[1] and Xiyuan Chen[1]**

[1] Department of Mathematics and Physics, Shijiazhuang Tiedao University, Shijiazhuang, China
[2] Department of Engineering Mechanics, Shijiazhuang Tiedao University, Shijiazhuang, China

* **Correspondence:** Email: wangqiubao12@sina.com.

**Abstract:** It is reasonable to use uncertain nonlinear differential equations to model systems that are subject to noise disturbances of unstable frequency, such as uncertain financial systems, biological population systems, infectious disease systems, and pharmacokinetic systems. Due to the coupling effect of nonlinearity and uncertainty, it is challenging to directly solve the responses of these equations. This paper addressed the challenge of studying the responses of these systems, especially the changes in steady-state behavior caused by parameter variations, known as "bifurcation" phenomena. We defined the concept of Hopf bifurcation in uncertain differential equations using cross-entropy and investigated the bifurcation phenomena in a class of second-order uncertain nonlinear differential equations. An efficient algorithm was designed to verify uncertain Hopf bifurcation and quantify the bifurcation threshold, with the validity of our definition confirmed through numerical simulations. This paper extended the classical Hopf bifurcation of ordinary differential equations to uncertain differential equations via the $\alpha$-path, thereby proposing a theoretical framework for uncertain bifurcation within uncertain dynamics.

**Keywords:** Hopf bifurcation; uncertain nonlinear differential equation; cross-entropy
**Mathematics Subject Classification:** 34A12, 47E05

## 1. Introduction

Nonlinear vibration is a critical area of study in the field of dynamics and has wide-ranging applications across various disciplines. The phenomenon of nonlinear vibration is observed in a variety of natural and man-made systems, including earthquakes, mechanical systems, and biological structures. In order to capture the essence of nonlinear vibrations, nonlinear differential equations are employed. These equations are fundamental to the field of mathematics and provide a mathematical framework to model and analyze the behavior of such complex systems. The solutions to these

equations can reveal important information about the system's response to various inputs, including its stability, resonance, and chaotic behavior. One of the key challenges in studying nonlinear vibrations is the presence of noise disturbances. Noise can come from various sources, such as environmental factors, manufacturing imperfections, or inherent uncertainties in the system's parameters. These disturbances can significantly affect the system's dynamics, complicating the accurate prediction of its behavior. To address this challenge, researchers have turned to the theories of stochastic calculus. By incorporating randomness into the models, stochastic calculus allows for the analysis of systems under the influence of noise. This approach is grounded in probability theory, which provides the necessary tools to quantify and understand the probabilistic nature of the system's response to noise. The framework of stochastic dynamic models has been instrumental in advancing our understanding of nonlinear vibrating systems. By considering the system as a stochastic process, researchers can account for the uncertainties and random fluctuations in the system's behavior. This has led to the development of sophisticated models that can accurately capture the complex interactions between the deterministic dynamics of the system and the stochastic influences of noise. The success of this approach is evident in its widespread application across various fields. In physics, stochastic models have been used to study phenomena such as turbulence and phase transitions. In finance, they have been applied to model the fluctuations in stock prices and other financial instruments. In biology, they have helped to understand the dynamics of complex biological systems, such as neural networks and ecosystems. The extensive development of stochastic dynamic models has yielded fruitful results, as evidenced by the numerous studies and publications on the topic [1–3]. The continued research in this area is crucial for further enhancing our ability to understand and predict the behavior of nonlinear vibrating systems under various conditions. This, in turn, can lead to improved designs and control strategies for engineering applications, as well as a deeper understanding of natural phenomena.

A prerequisite for the application of stochastic theory is that the distribution function closely approximates the actual frequency based on a sufficient amount of data. However, in most cases, the frequency is unstable, such as stock fluctuations, infectious disease models, etc., where most of the time the frequency is unstable when data is scarce, for example, during military conflicts, extreme weather conditions, or even rumors, where only limited or no data is available [4]. In practical problems where sample data is insufficient or non-existent, an expert's level of confidence can be obtained by consulting a domain expert. It is important to note that the degree of belief, influenced by human conservatism and subjectivity, as demonstrated by Kahneman and Tversky [5], can significantly differ from the true frequency. Liu [6] highlighted that employing probability theory to handle experts'degrees of belief may lead to counterintuitive outcomes, which has prompted the development of uncertainty theory.

Furthermore, stochastic differential equation models often exhibit paradoxes. For instance, when considering heat sources that are frequently influenced by noise, Walsh [7] proposed a stochastic heat equation driven by the Wiener process. Subsequent studies by Chow [8], Peter [9], Peszat and Zabczyk [10], and other researchers have explored the stochastic heat equation. However, it raises doubts about the appropriateness of employing random heat equations to depict actual heat conduction processes. Many scholars have recognized the presence of paradoxes in modeling with stochastic differential equations. Yang and Yao introduced another related to the stochastic heat equation [11], both highlighting the impracticality of using random heat equations to accurately describe actual heat conduction. The essence of these paradoxes is rooted in the fact that the variance of the independent increments of Brownian motion corresponds to the time interval, that is, $B(t + \Delta t) - B(t) \sim N(0, \Delta t)$. In

response to these challenges, Liu proposed an uncertainty theory founded on four axioms: normality axiom, duality axiom, subadditivity axiom, and product axiom [6]. Liu emphasized that, in the absence of known frequency, substituting the uncertain differential equations driven by the Wiener process with the uncertain Liu process can enhance the simulation of real-world phenomena and avoid the aforementioned paradoxes.

Liu [6] demonstrated that due to personal preferences and cognitive limitations, individuals tend to conservatively estimate belief degrees for uncertain events, resulting in a larger interval of belief degrees. In situations where decision information is limited, relying solely on probability theory may not lead to reasonable decisions. Additionally, the subjectivity of belief degrees makes the imposition of objective attributes through probability inappropriate, diverging from actual circumstances. Thus, it is more appropriate to use uncertainty theory to describe reliability when system information is limited.

Liu [6] established uncertainty theory based on uncertainty measures and defined uncertain variables. To better characterize uncertain variables, Liu [6] introduced the concept of uncertain distribution. Furthermore, Peng and Iwamura [12] proposed sufficient and necessary conditions for the existence of uncertain distributions. Liu [13] introduced the concept of independence for uncertain variables and developed the uncertainty calculus theory for the Liu process. Liu [14]proposed a novel uncertain process as an alternative to the Wiener process, known as the Lipschitz continuous uncertain process with steady independent normal increments. In 2008, Liu [15] pioneered the concept of UDEs (uncertain differential equations) based on the Liu process, which became a fundamental tool for handling uncertain dynamic systems. Subsequently, Chen and Liu [16] proved the existence and uniqueness theorem for solutions of UDEs under linear growth and Lipschitz continuity conditions. This work sparked further investigations by numerous researchers. For instance, Yao [17] explored various stability properties, while Yao [18] and Liu [19] provided analytical solutions for certain types of UDEs. Additionally, researchers have investigated stability in different forms for universal uncertain differential equations [20, 21], and others have delved into parameter estimation [22, 23]. Recently, researchers have begun to extend UDEs to higher-order cases. For example, Wang et al. [24] systematically studied second-order and a class of higher-order UDEs. Thereby further refining the analytical framework for higher-order uncertain systems. However, finding analytical solutions remains challenging for universal UDEs.

Fortunately, Yao proposed the Yao-Chen formula, which, in collaboration with Chen, establishes the relationship between UDEs and ordinary differential equations(ODEs) [25]. Specifically, the inverse distribution function of the solutions of UDEs is determined by the solutions of a family of ODEs. This formulation enables numerical simulations and related studies of UDEs. Building upon this formula, Yao introduced the Euler method to solve UDEs [26]. Subsequently, various numerical methods have been devised, including the Runge-Kutta and Adams methods by Yang [27, 28], the Adams-Simpson method by Wang [29], and the Milne method by Gao [30], to obtain numerical solutions for UDEs. Thanks to the Lipschitz continuity property inherent in the Liu process, the existence and uniqueness theorem established for solutions of deterministic differential equations can be extended to UDEs. As a result, significant advancements have been made both in theoretical understanding and practical applications of UDEs.With the advancements in high-order UDEs, Yao [31] introduced high-order UDEs as a tool to deal with high-order uncertain differentiable systems in 2016. However, obtaining analytical solutions for universal UDEs remains a challenging task. To address this, Yao [31] introduced the Euler method, Hou [32] proposed the Adams-Simpson method, Jin [33] presented

the Runge-Kutta method, and Kuang [34] proposed the improved Milne-Hamming method and other numerical techniques to obtain numerical solutions.

While obtaining analytical solutions for higher-order NDEs (nonlinear differential equations) is difficult, substantial progress has been made in understanding their dynamical properties, particularly bifurcation and chaos [35–37]. Based on these developments, significant achievements have also been made in studying the bifurcation of stochastic differential equations [38–40]. In light of these findings, researchers have explored whether UNDEs(uncertain nonlinear differential equations) have similar counterparts to stochastic nonlinear differential equations(SNDEs), such as bifurcation and chaos, in the context of uncertainty theory. This paper proposes to study "uncertain bifurcation" based on cross-entropy. The study draws the definition of cross-entropy in uncertain processes [41]. The aim of this study is to extend research on NDEs to the field of UNDEs, with a particular focus on bifurcation. While this paper provides only a preliminary exploration, it offers a quantitative definition of an uncertain Hopf bifurcation.

The structure of this paper is given as follows: Section 2 reviews related concepts and conclusions of the uncertainty theory; Section 3 gives the concept of Hopf bifurcation for UNDEs; Section 4 designs an efficient algorithm to illustrate the rationality of the proposed concept and method; Section 5 gives the main conclusions.

## 2. Preliminaries

In this section, this paper will introduce some basic concepts, cross-entropy and other related concepts of uncertainty theory.

**Definition 2.1** (Liu 2024 [6]). *The uncertainty distribution* $\Phi$ *of an uncertain variable* $\xi$ *is defined by*

$$\Phi(x) = \mathcal{M}\{\xi \leq x\}$$

*for any real number x.*

**Definition 2.2** (Liu 2024 [6]). *An uncertainty distribution* $\Phi(x)$ *is said to be regular if it is a continuous and strictly increasing function with respect to x at which* $0 < \Phi(x) < 1$ *, and*

$$\lim_{x\to-\infty} \Phi(x) = 0, \lim_{x\to+\infty} \Phi(x) = 1.$$

**Definition 2.3** (Liu 2024 [6]). *Let* $\xi$ *be an uncertain variable with regular uncertainty distribution* $\Phi(x)$*. Then, the inverse function* $\Phi^{-1}(\alpha)$ *is called the inverse uncertainty distribution of* $\xi$ *.*

Following that, the definition of uncertain process will be given, which is composed of a series of uncertain variables indexed by time $t$ as follows.

**Definition 2.4** (Liu 2024 [6]). *An uncertain process* $C_t$ *is said to be a Liu process if*

*(i)* $C_0 = 0$ *and almost all sample paths are Lipschitz continuous,*

*(ii)* $C_t$ *has stationary and independent increments,*

*(iii) every increment* $C_{s+t} - C_s$ *is a normal uncertain variable with expected value* 0 *and variance* $t^2$*.*

**Theorem 2.1** (Chen-Liu Existence and Uniqueness Theorem [6]). *The UDE*

$$\mathrm{d}X_t = f(t, X_t)\mathrm{d}t + g(t, X_t)\mathrm{d}C_t$$

*has a unique solution if the functions $f(t,x)$ and $g(t,x)$ satisfy the linear growth condition*

$$|f(t,x)| + |g(t,x)| \leq L(1+|x|), \forall x \in \Re, t \geq 0$$

*and Lipschitz condition*

$$|f(t,x) - f(t,y)| + |g(t,x) - g(t,y)| \leq L(|x-y|), \forall x, y \in \Re, t \geq 0.$$

*Without loss of generality, suppose L. Moreover, the solution is sample-continuous.*

**Theorem 2.2** (Yao-Chen [6])**.** *Let $\alpha$ be a number between* 0 *and* 1*. An UDE*

$$\mathrm{d}X_t = f(t, X_t)\mathrm{d}t + g(t, X_t)\mathrm{d}C_t$$

*is said to have an $\alpha$-path $X_t^\alpha$ if it solves the corresponding ODE*

$$\mathrm{d}X_t^\alpha = f(t, X_t^\alpha)\mathrm{d}t + |g(t, X_t^\alpha)|\Phi^{-1}(\alpha)\mathrm{d}t$$

*where $\Phi^{-1}(\alpha)$ is the inverse standard normal uncertainty distribution, i.e.,*

$$\Phi^{-1}(\alpha) = \frac{\sqrt{3}}{\pi}\ln\frac{\alpha}{1-\alpha}.$$

According to Theorem 2.2, the inverse distribution of the UDE can be determined. Do such second-order UDEs also have conclusions similar to Theorem 2.2? We discussed this issue in another article and found that second-order differential equations have similar conclusions.

**Definition 2.5.** *Let $\alpha$ be a number between* 0 *and* 1*. An UDE*

$$\begin{cases} \frac{\mathrm{d}^2X_t}{\mathrm{d}t^2} = f(t, X_t, \frac{\mathrm{d}X_t}{\mathrm{d}t}) + g(t, X_t, \frac{\mathrm{d}X_t}{\mathrm{d}t})\frac{\mathrm{d}C_t}{\mathrm{d}t}, \\ X_t\Big|_{t=0} = X_0, \frac{\mathrm{d}X_t}{\mathrm{d}t}\Big|_{t=0} = Y_0, \end{cases}$$

*is said to have an $\alpha$-path $X_t^\alpha$ if it solves the corresponding ODE*

$$\begin{cases} \frac{\mathrm{d}^2X_t^\alpha}{\mathrm{d}t^2} = f(t, X_t^\alpha, \frac{\mathrm{d}X_t^\alpha}{\mathrm{d}t}) + |g(t, X_t^\alpha, \frac{\mathrm{d}X_t^\alpha}{\mathrm{d}t})|\Phi^{-1}(\alpha), \\ X_t^\alpha\Big|_{t=0} = X_0, \frac{\mathrm{d}X_t^\alpha}{\mathrm{d}t}\Big|_{t=0} = Y_0, \end{cases}$$

*where $\Phi^{-1}(\alpha)$ is the inverse standard normal uncertainty distribution, i.e.,*

$$\Phi^{-1}(\alpha) = \frac{\sqrt{3}}{\pi}\ln\frac{\alpha}{1-\alpha}.$$

**Remark 2.1.** *The definition of a second-order UDEs corresponds to a determinate equations whose solution, when certain conditions are met for $f$ and $g$, is the inverse distribution of the UDEs. This conclusion allows us to study UDEs through the research methods of determinate equations.*

Entropy is used to measure the uncertainty associated with a variable whose value cannot be exactly predicated in information sciences. The definition of cross-entropy of uncertain variables was proposed by Gao [41].

**Definition 2.6** (Xin Gao, 2018 [41]). *Let $\xi$ and $\eta$ be two uncertain variables with uncertainty distributions $\Phi$ and $\Psi$, respectively. Then, the cross-entropy of $\xi$ from $\eta$ is defined by*

$$D[\xi, \eta] = \int_{-\infty}^{+\infty} |\Phi(x) - \Psi(x)| \mathrm{d}x. \tag{2.1}$$

**Theorem 2.3** (Xin Gao, 2018 [41]). *Let $\xi$ and $\eta$ be two uncertain variables with regular uncertainty distributions $\Phi$ and $\Psi$ , respectively. Then, the cross-entropy of $\xi$ and $\eta$ is*

$$D[\xi, \eta] = \int_{0}^{1} |\Phi^{-1}(\alpha) - \Psi^{-1}(\alpha)| \mathrm{d}\alpha. \tag{2.2}$$

## 3. Hopf bifurcation of uncertain differential equtions

The Hopf bifurcation is an important feature of nonlinear dynamical systems. How can the bifurcation in uncertain nonlinear systems be described and measured? This section aims to intuitively understand the Hopf bifurcation of uncertain nonlinear eqution, starting with a simple example. According to the characteristics of deterministic systems, at least a second-order system is required to potentially produce a Hopf bifurcation. Therefore, the discussion begins with a simple second-order UDE.

$$\ddot{x}_t + \omega^2 x_t = \varepsilon[f(t, x_t, \dot{x}_t, \xi) + g(t, x_t, \dot{x}_t, \xi)\dot{C}_t], \tag{3.1}$$

where $f(t, x_t, \dot{x}_t, \xi)$,$g(t, x_t, \dot{x}_t, \xi)$ are two given functions, $C_t$ is a normal Liu process, $\varepsilon$ is an arbitrarily small positive number, and $\xi$ represents the physical parameter of the system.

$$\Phi^{-1}(\alpha) = \frac{\sqrt{3}}{\pi} \ln \frac{\alpha}{1-\alpha}$$

is the inverse uncertainty distribution of standard normal uncertain variables.

According to Definition 2.5, we have

$$\ddot{x}_t^{\alpha} + \omega^2 x_t^{\alpha} = \varepsilon[f(t, x_t^{\alpha}, \dot{x}_t^{\alpha}, \xi) + |g(t, x_t^{\alpha}, \dot{x}_t^{\alpha}, \xi)|\Phi^{-1}(\alpha)]. \tag{3.2}$$

Obviously, Eq (3.2) is a family of deterministic equations, and its solution determines the inverse distribution of Eq (3.1). Next, we discuss the conditions for a Hopf bifurcation about the deterministic equation (3.2). Let

$$\begin{aligned} x_t^{\alpha} &= A^{\alpha} \cos \varphi, \\ \dot{x}_t^{\alpha} &= -A^{\alpha} \omega \sin \varphi, \\ \varphi &= \omega t + \theta^{\alpha}. \end{aligned} \tag{3.3}$$

Using the average theory

$$\dot{A^{\alpha}} = -\varepsilon F(A^{\alpha}, \theta^{\alpha}, t, \xi) \sin \varphi, \tag{3.4a}$$

$$A^{\alpha}\dot{\theta^{\alpha}} = -\varepsilon F(A^{\alpha}, \theta^{\alpha}, t, \xi) \cos \varphi, \tag{3.4b}$$

where

$$\begin{aligned} F(A^\alpha, \theta^\alpha, t, \xi) =& f(t, A^\alpha \cos\varphi, -A^\alpha \omega \sin\varphi, \xi) \\ &+ |g(t, A^\alpha \cos\varphi, -A^\alpha \omega \sin\varphi, \xi)| \Phi^{-1}(\alpha). \end{aligned} \tag{3.5}$$

Averaging the formula (3.4a–3.4b) in the period $[0, 2\pi]$, we get:

$$\dot{A^\alpha} = -\frac{\varepsilon}{2\pi} \int_0^{2\pi} F(A^\alpha, \theta^\alpha, t, \xi) \sin\varphi \mathrm{d}\varphi, \tag{3.6a}$$

$$A^\alpha \dot{\theta^\alpha} = -\frac{\varepsilon}{2\omega\pi} \int_0^{2\pi} F(A^\alpha, \theta^\alpha, t, \xi) \cos\varphi \mathrm{d}\varphi. \tag{3.6b}$$

According to Definition 2.5, an uncertain nonlinear differential equation(UNDE) (3.1) can be transformed into a deterministic equation (3.2). The Hopf bifurcation of the deterministic nonlinear equation is a phenomenon of dynamic system bifurcation, where the equilibrium point of the system transitions from a stable state to an unstable state as the system parameters pass through a critical value, simultaneously giving rise to a periodic solution (i.e., a limit cycle). This type of bifurcation is usually associated with the system's transition from a stationary state to an oscillatory state.

According to the Hopf bifurcation theory of deterministic systems, the existence of periodic solutions can be determined using the averaging method.The stability of the limit cycle of Eq (3.2) in the vicinity of $(x, \dot{x}) = (0, 0)$ can be analyzed in the following ways:

(1) As the parameter changes, when the parameter $\xi$ passes through $\xi_c$, it will result in $\dot{A}^\alpha$ going from $\dot{A}^\alpha > 0$ to $\dot{A}^\alpha < 0$, and a subcritical Hopf bifurcation occurs. The solution changes from an unstable focus to an asymptotically stable focus and produces an unstable periodic solution.

(2) As the parameter changes, when the parameter $\xi$ passes through $\xi_c$, it will result in $\dot{A}^\alpha$ going from $\dot{A}^\alpha < 0$ to $\dot{A}^\alpha > 0$, and a supercritical Hopf bifurcation occurs. The solution changes from an asymptotically stable focus to an unstable focus, and an asymptotically stable limit cycle is generated.

In Eq (3.2), if for any $\forall\ 0 < \alpha < 1$ , each corresponding determined system undergoes a Hopf bifurcation at the same $\xi_c$ and a limit cycle with a period of $T$ appears. Hence, for $\forall\ t, \alpha$, the inverse distribution of the solution of system (3.2) at time $t$ satisfies $\phi_t^{-1}(\alpha) = x_t^\alpha$, $\phi_{t+T}^{-1}(\alpha) = x_{t+T}^\alpha$. Given the assumption from the previous context that $x_t^\alpha = x_{t+T}^\alpha$, it follows that $\phi_t^{-1}(\alpha) = \phi_{t+T}^{-1}(\alpha)$, which implies that the inverse distribution is a periodic function with a period of $T$. Is it possible to describe the state transitions of the uncertain equation (3.1) using the periodicity of $\phi_t^{-1}(\alpha)$? When $\varepsilon = 0$, $T = \frac{2\pi}{\omega}$. However, since we are studying a nonlinear system where $\varepsilon \neq 0$, the values of $\xi_c$ and $T$ differ from those in the determined system. From the previous derivations, it can be observed that for each $\alpha$-path in the nonlinear system, the corresponding values of $\xi_c$ and $T$ may not be the same, when $\varepsilon \neq 0$, $T(\alpha_1) = T(\alpha_2) + O(\varepsilon), \xi_c(\alpha) = \xi_c(\alpha_2) + O(\varepsilon)$. $\phi_t^{-1}(\alpha)$ and $\phi_{t+T}^{-1}(\alpha)$ are not necessarily equal, and they may differ by an infinitesimal of the same order as $\varepsilon$. However, even though they are not strictly equal, the states of the uncertain system are different when $\xi > \xi_c$ and $\xi < \xi_c$, and the behavior of the inverse distribution function is also different, where $\xi_c$ is the supremum of $\xi_c(\alpha)$. Therefore, to describe the state transitions of an uncertain system, we introduce the concept of cross-entropy to measure the state transitions of the uncertain system.

**Definition 3.1** (Cross-entropy of the reference-containing system)**.** *A containing parameters $\xi \in \Re$ UNDEs*

$$\frac{\mathrm{d}^n X_t}{\mathrm{d}t^n} = f(t, X_t, \frac{\mathrm{d}X_t}{\mathrm{d}t}, \cdots, \frac{\mathrm{d}^{n-1} X_t}{\mathrm{d}t^{n-1}}; \xi) + g(t, X_t, \frac{\mathrm{d}X_t}{\mathrm{d}t}, \cdots, \frac{\mathrm{d}^{n-1} X_t}{\mathrm{d}t^{n-1}}; \xi) \frac{\mathrm{d}C_t}{\mathrm{d}t}, \tag{3.7}$$

*where*

$$f(t, X_t, \frac{\mathrm{d}X_t}{\mathrm{d}t}, \cdots \frac{\mathrm{d}^{n-1}X_t}{\mathrm{d}t^{n-1}}; \xi),$$

*and*

$$g(t, X_t, \frac{\mathrm{d}X_t}{\mathrm{d}t}, \cdots \frac{\mathrm{d}^{n-1}X_t}{\mathrm{d}t^{n-1}}; \xi),$$

*are measurable functions, and $C_t$ is a Liu process. A solution is an uncertain process $X_t$ that satisfies (3.7) identically in t. Then, define the function*

$$\boldsymbol{H}(\xi, t, t+\Delta t) = \int_0^1 \left|\Phi^{-1}(\alpha; \xi, t) - \Phi^{-1}(\alpha; \xi, t+\Delta t)\right| \mathrm{d}\alpha \tag{3.8}$$

*as the parameter-containing cross-entropy of the (3.7) solution at t and $t + \Delta t$.*

**Remark 3.1.** *The solution of (3.7) is an uncertain process. When the time t is determined, the uncertain process becomes an uncertain variable, so two uncertain variables given time t and $t+\Delta t$ are obtained. In essence, the parameter-containing cross entropy at time t and $t+\Delta t$ in (3.8) is the same cross entropy as in the literature [41].*

**Remark 3.2.** *If $\exists \underline{t}(\xi)$, when $t > \underline{t}(\xi)$, for $\forall \Delta t$, $\boldsymbol{H}(\xi, t, t+\Delta t) = 0$, indicating that the uncertainty process stabilizes, i.e., the inverse distribution of $X_t$ is invariant with respect to time t. This is similar to the existence of gradually stable attractors, which gives implications for our definition of uncertainty bifurcation.*

**Definition 3.2** (Hopf bifurcation)**.** *Considering the UNDEs (3.7) when $\xi < \xi_c$, $\forall \varepsilon > 0, \forall \Delta t > 0, \exists \underline{t}(\xi, \varepsilon)$, has*

$$\boldsymbol{H}(\xi, t, t+\Delta t) < \varepsilon, t > \underline{t}(\xi, \varepsilon), \tag{3.9a}$$

*when $\xi > \xi_c$, $\exists m \in Z$, $\exists \bar{t}(\xi)$, $\exists T(\xi) > 0$, satisfied*

$$\begin{aligned} &\boldsymbol{H}(\xi, t, t+T(\xi, \varepsilon)) < \varepsilon, \\ &\boldsymbol{H}(\xi, t, t+\frac{1}{2}T(\xi, \varepsilon)) > 10^m \varepsilon, t > \bar{t}(\xi, \varepsilon). \end{aligned} \tag{3.9b}$$

*When (3.9a) (3.9b) are satisfied, the parameter-containing $\xi$ UNDEs (3.7) at $\xi = \xi_c$ experience an uncertain Hopf bifurcation (m-Hopf bifurcation).*

**Remark 3.3.** *It is defined as "a kind of quantification" bifurcation, which is mainly reflected in m. In general, the larger the value of m, the more pronounced the state transitions in the system.*

**Remark 3.4.** *In practice, the verification of definition (3.9a) is difficult. (Due to the arbitrariness of the time interval $\Delta t$, which makes us want to verify the incomputable function $\boldsymbol{H}(\xi, t, t+\Delta t)$.) Using the density of rational numbers, for any arbitrary t, we seek a sequence $t_i$ that tends to t as a limit, such that $\boldsymbol{H}(\xi, t_i, t_i+\Delta t)$ tends to $\boldsymbol{H}(\xi, t, t+\Delta t)$ as a limit. Therefore, we adopt the following plan: For a given $\xi, \varepsilon$, select a $\Delta t$, choose a large enough $n \in Z$ (say n=1000), select a moment $t > \underline{t}(\xi, \varepsilon)$, let $t = t_0 + i\Delta t, i = 0, 1, 2, \ldots, n$, let $\boldsymbol{H_M}(\xi(n)) = \max_{i=1,2,\ldots,n-1} \int_0^1 \left|\Phi^{-1}(\alpha; \xi, t_i) - \Phi^{-1}(\alpha; \xi, t_i+\Delta t)\right| d\alpha$, and use $\boldsymbol{H_M}(\xi(n)) < \varepsilon$ instead of the two inequalities in the definition (3.9a) to judge. In fact, $\boldsymbol{H_M}(\xi(n))$ still needs to adopt appropriate algorithms. See algorithm 1 for details.*

**Remark 3.5.** *Because of the various quantifications and approximations described above, the "bifurcation value" we obtain is often not a value, but an interval with a smaller range of values. When passing through this interval, the system completes the state transition, as shown in Figure 1 for details.*

**Remark 3.6.** *The characteristic of Hopf bifurcation in determined system is the transition from asymptotically stable to periodic solution of the limit cycle (or vice versa). Similarly, we define the Hopf bifurcation in uncertain system in terms of the state transitions of its inverse distribution. (3.9a) means that when t is sufficiently large, the inverse distribution of the uncertain system does not change with t, which is referred to as "asymptotically stable"; (3.9b) means that the inverse distribution of the uncertain system is "periodic". They reflect the dynamic transition behavior of the uncertain system.*

If the UNDEs satisfies the aforementioned two conditions (3.9a) (3.9b) during parameter changes, there is reason to believe that an uncertain system generates some form of Hopf bifurcation with a confidence level of 1. This is defined as a supercritical Hopf bifurcation similar to deterministic systems, where a limit cycle is generated from a steady-state solution. Conversely, when parameters increase and the limit cycle disappears, this is similar to a subcritical Hopf bifurcation in deterministic systems, and is considered a Hopf bifurcation in uncertain systems. In order to more clearly demonstrate the dynamical behavior of uncertain systems that satisfy the conditions, we designed an effective algorithm for visualization and provided numerical analysis of the existence of bifurcations in Section 4.

## 4. Algorithm design and numerical simulation

This part provides numerical experiments of the improved order 4 Runge-Kutta method(RK-4), additionally, the effectiveness and efficiency of which will be demonstrated. The equation is

$$\ddot{x} + \omega^2 x + \varepsilon\left[\left(\xi + \gamma x^2\right)\dot{x} - F_0 \cos \Omega t + g(t, x)\frac{\mathrm{d}C_t}{\mathrm{d}t}\right] = 0. \tag{4.1}$$

According to Definition 2.5, the $\alpha - path(0 < \alpha < 1)$ corresponds to the equation of system(4.1)

$$\ddot{x}_t^\alpha + \omega^2 x_t^\alpha = \varepsilon\left[F_0 \cos \Omega t - (\xi + \gamma(x_t^\alpha)^2)\dot{x}_t^\alpha + |g(t, x_t^\alpha, \dot{x}_t^\alpha)|\frac{\sqrt{3}}{\pi} \ln \frac{\alpha}{1-\alpha}\right], \tag{4.2}$$

where $f(t, x, \dot{x}) = F_0 \cos \Omega t - (\xi + \gamma x^2)\dot{x}, g(t, x) = 1$.

### *4.1. Algorithm of improved order 4 Runge-Kutta method*

Based on the $\alpha$-path in formula (4.2), discretizing $\alpha$ from 0 to 1 as $\alpha_1, \alpha_2, \ldots, \alpha_p$ will lead to an exponential increase in the time complexity of finding the $\alpha$-path. Consequently, this paper examines the properties of uncertain distributions by integrating $\alpha$ using formulas (4.2). This presents a conflict between accuracy and computational complexity: to ensure accuracy, $p$ needs to be as large as possible, which is one issue. Furthermore, the high spatial complexity presents another challenge. As shown in the example below, the convergence of the $\alpha$-path near the Hopf bifurcation point is very slow, requiring longer simulation times to discover the asymptotic stable trend ($t > e^4 s$). Therefore, a large amount of memory is required to store the results of the time sequence. Each $\alpha$-path needs to store a large amount of time data, making storage a huge challenge.

**Algorithm 1** Calculating the Threshold $\boldsymbol{H_M}(\xi)$

Initialization of a bifurcation parameter sequence $\xi_j$, $j = 1, 2, \ldots, m$; given a time range $t \in (0, t_{max})$ and a time interval $\Delta t$;
Discretize time into $t_i = t_0 + i\Delta t, i = 0, 1, 2, \ldots, n$.
$n = t_{max}/\Delta t$;
Discretize uncertain measure $\boldsymbol{\alpha} \in (0, 1)$ with intervals of h as $\alpha_k = kh, k = 1, 2, \ldots, p = (1 - h)/h$.
**for** $\xi = \xi_1, \xi_2, \ldots, \xi_m$ **do**
    **for** $\alpha = \alpha_1, \alpha_2, \ldots, \alpha_p$ **do**
        Calculate $\alpha$-path through ODE:
$\mathrm{d}X_t^{\alpha_k} = f(t, X_t^{\alpha_k})\mathrm{d}t+$
$|g(t, X_t^{\alpha_k})|\Phi^{-1}(\alpha_k)\mathrm{d}t, \quad X_0^{\alpha_k} = X_0$
        Obtain the inverse uncertainty distribution $\Phi^{-1}(\alpha_k; \xi, t_i)$ of $X_t^{\alpha_k}$ through Theroem x.
    **end for**
    Numerical integration using the trapezoidal method:

$$\boldsymbol{H_M}(\xi_j) = \max_{i=1,2,\ldots,n-1} \sum_{k=1}^{p-1} (|\Phi^{-1}(\alpha_k; \xi, t_i) - \Phi^{-1}(\alpha_k; \xi, t_{i+1})| + |\Phi^{-1}(\alpha_{k+1}; \xi, t_i) - \Phi^{-1}(\alpha_{k+1}; \xi, t_{i+1})|)h/2$$

**end for**

**Output:** $\boldsymbol{H_M}(\xi_j)$

**Algorithm 2** Simulating the $\alpha$-path

For any differential equation, we first transform it into a system of first-order differential equations.Given a $\alpha$-path through ODE:
$\mathrm{d}X_t^{\alpha} = f(t, X_t^{\alpha})\mathrm{d}t + |g(t, X_t^{\alpha})|\Phi^{-1}(\alpha)\mathrm{d}t,$
$X_0^{\alpha} = X_0 = (X_0^1, X_0^2, \ldots, X_0^m)$
The moment $t_{begin}$ represents the commencement of data storage.
Discretize time $t \in (0, t_{max})$ into $t_i = t_0 + i\Delta t,$
$i = 0, 1, 2, \ldots, n.n = t_{max}/\Delta t;$
Discretize uncertain measure $\boldsymbol{\alpha} \in (0, 1)$ with intervals of $h$ as $\alpha_k = kh, k = 1, 2, \ldots, p = (1 - h)/h,$
$\boldsymbol{\alpha} = (\alpha_1, \alpha_2, \ldots, \alpha_p).$
Construct matrix $X = I_{k\times 1}X_0$, where $I$ is a vector with all elements of 1, it is equivalent to copying $X_0$ to k rows. Construct matrix
$\Phi^{-1}(\boldsymbol{\alpha}) = (\Phi^{-1}(\alpha_1), \Phi^{-1}(\alpha_1), \ldots, \Phi^{-1}(\alpha_k))^T.$
**for** $t = t_i, i = 1, 2, \ldots, n$ **do**
    $K_1 = f(t, X) + |g(t, X)| \odot \Phi^{-1}(\boldsymbol{\alpha})$
    $K_2 = f(t + \frac{\Delta t}{2}, X + \frac{K_1}{2}) + |g(t + \frac{\Delta t}{2}, X + \frac{K_1}{2})| \odot \Phi^{-1}(\boldsymbol{\alpha})$
    $K_3 = f(t + \frac{\Delta t}{2}, X + \frac{K_2}{2}) + |g(t + \frac{\Delta t}{2}, X + \frac{K_2}{2})| \odot \Phi^{-1}(\boldsymbol{\alpha})$
    $K_4 = f(t + \Delta t, X + K_3) + |g(t + \Delta t, X + K_3)| \odot \Phi^{-1}(\boldsymbol{\alpha})$
    $X = X + \frac{1}{6}(K_1 + 2K_2 + 2K_3 + K_4)\Delta t$
    **if** $t > t_{begin}$ **then**
        save X to res.
    **end if**
**end for**

**Output:** res

Taking the numerical experiment in this paper as an example, in the case of $n = 99, \xi : -0.5 : 0.005 : 0.5, t = 2 * 10^4$, and step=0.01, as shown in Tables 1 and 2, if the traditional ode45 solver is used to solve each $\alpha$-path, it requires 1.49G of memory, which is too expensive. Therefore, this paper designs an order4 $\alpha$-path Runge-Kutta algorithm, which introduces the discrete sequence of the $\alpha$-path into the RK-4 algorithm, taking advantage of the efficiency of vector operations on computers to improve computational efficiency by up to 100 times. At the same time, during the process of solving the $\alpha$-path in the RK algorithm, the convergence of the $\alpha$-path is judged to truncate the solution sequence and only retain part of the time sequence, reducing the memory requirement to below 20M. This allows a regular computer to obtain simulation results within 1 hour.

**Table 1.** Time and space complexity comparisons.

| | ODE45 | order 4 $\alpha$-path Runge-Kutta |
|---|---|---|
| Time complexity | $O(k^{mp})$ | $O(k^m)$ |
| Spatial complexity | $O(n)$ | $O(1)$ |

**Table 2.** Specific numerical comparisons.

| | ODE45 | order 4 $\alpha$-path Runge-Kutta |
|---|---|---|
| Time | 47255s | 9335s |
| Spatial | 1.49G | 18M |

### *4.2. Application of improved order 4 Runge-Kutta method*

Using parameters $\xi$ and $\gamma$ to represent the nonlinear damping $\xi + \gamma x^2$ in Eq (4.1), and applying the averaging method described in the third section to Eq (4.2), the average equation of the system can be obtained.

$$\dot{A^\alpha} = -\epsilon F(A^\alpha, \theta^\alpha, t, \xi) \sin\varphi, \tag{4.3a}$$

$$A^\alpha \dot{\theta^\alpha} = -\epsilon F(A^\alpha, \theta^\alpha, t, \xi) \cos\varphi, \tag{4.3b}$$

where

$$\begin{aligned} F(A^\alpha, \theta^\alpha, t, \xi, \gamma) =& A^\alpha(\xi + \gamma {A^\alpha}^2 \cos^2\varphi) \sin\varphi + F_0 \cos\Omega t \\ &+ |g(t, A^\alpha \cos\varphi, -A\omega \sin\varphi, \xi, \gamma)| \frac{\sqrt{3}}{\pi} \ln\frac{\alpha}{1-\alpha}. \end{aligned} \tag{4.4}$$

Averaging the formula (4.3a–4.3b) in the period $[0, 2\pi]$, we get:

$$\dot{A^\alpha} = -\frac{F_0}{4\pi}\int_0^{2\pi} \sin(\varphi - \Omega t)\mathrm{d}\varphi - \frac{1}{2}(A^\alpha \xi + \frac{{A^\alpha}^3 \gamma}{4}), \tag{4.5a}$$

$$A^\alpha \dot{\theta^\alpha} = -\frac{F_0}{4\pi}\int_0^{2\pi} \cos(\varphi - \Omega t)\mathrm{d}\varphi. \tag{4.5b}$$

The use of the $\alpha$-path average equation allows for the determination of bifurcation patterns along the $\alpha$-path.

1) $\gamma > 0$: Figure 1 is the bifurcation diagram of Eq (4.2). Zone 1 represents a stable limit cycle, zone 2 depicts a gradually decreasing limit cycle, and zone 3 signifies asymptotic stability. For $\gamma > 0$, the $\alpha$-path exhibits characteristics akin to a supercritical Hopf bifurcation. As the bifurcation parameter changes, the system transitions from a stable limit cycle to asymptotic stability gradually, with zone 2 indicating the shrinking of the limit cycle. Furthermore, due to the slow decay near the bifurcation point, it is challenging to discern small-amplitude periodic motion from asymptotic stability accurately through numerical methods. Hence, the boundary between periodic motion and asymptotic stability is not distinctly defined.

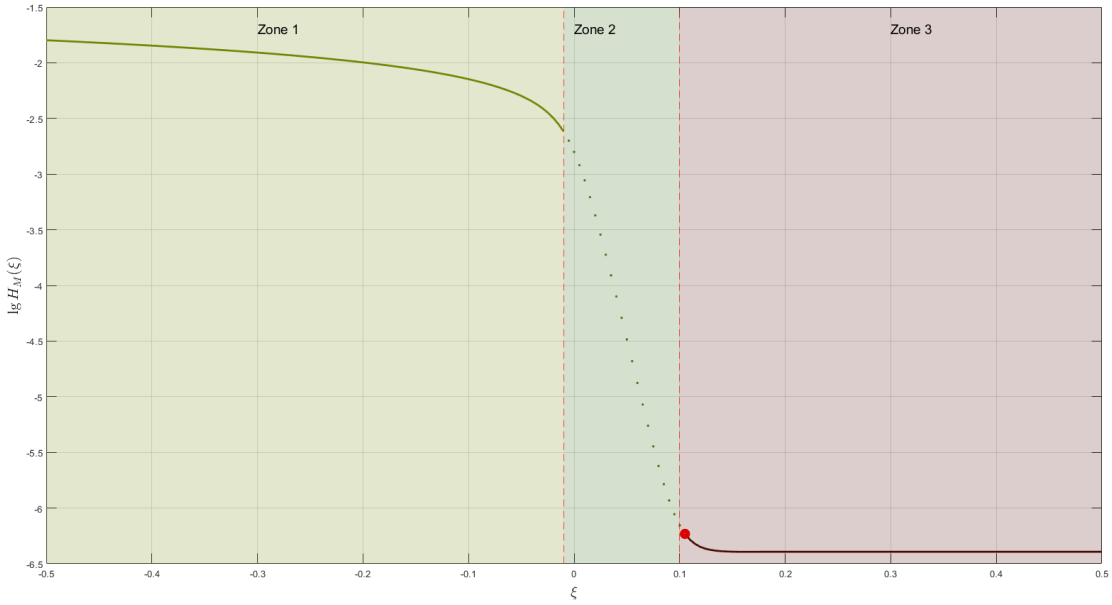


**Figure 1.** Bifurcation diagram of Eq (4.1), where $\Delta t = 0.01; n = 2 \times 10^6$.

In Figure 2, for the parameter values $\xi = [-0.1, 0, 0.1, 0.2]$, the $\alpha$ -path exhibits a gradual decrease in amplitude leading to convergence.

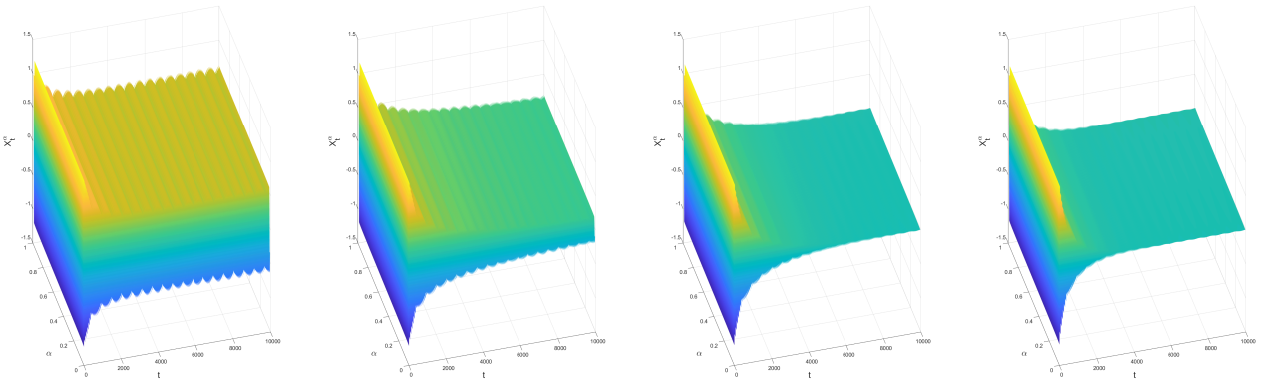

**(a)** $\xi = -0.1$ **(b)** $\xi = 0$ **(c)** $\xi = 0.1$ **(d)** $\xi = 0.2$

**Figure 2.** The 3D plot of the $\alpha$-path depicts the behavior of the path for the parameter values $\xi = [-0.1, 0, 0.1, 0.2]$. The plot reveals a uniform tendency in all $\alpha$-path as $\xi$ increases, transitioning from periodic motion to gradual decay and ultimately to asymptotic stability.

Figures 3 ($\alpha$=0.01), 4 ($\alpha$=0.45), and 5 ($\alpha$=0.99) display different $\alpha$-paths, with their two-dimensional trajectories providing important findings that complement the three-dimensional representation in Figure 2 . All visualization results consistently identify $\xi \approx 0.1$ as a critical bifurcation point where the system undergoes a qualitative transition from periodic oscillation to asymptotic stability. This bifurcation behavior remains remarkably consistent across different $\alpha$ values, indicating that the parameter $\xi$ is the primary determinant triggering this fundamental behavioral transformation. However, they exhibit significantly different convergence characteristics: the trajectory in Figure 4 shows more pronounced transient oscillations and slower convergence speed after bifurcation, while the path in Figure 5 demonstrates a significantly accelerated stabilization process.

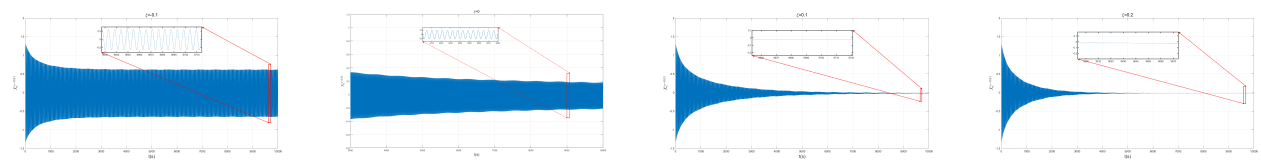

**(a)** $\xi = -0.1$ **(b)** $\xi = 0$ **(c)** $\xi = 0.1$ **(d)** $\xi = 0.2$

**Figure 3.** The 2D plot of the $\alpha$ -path for the parameter values $\xi = [-0.1, 0, 0.1, 0.2]$ at $\alpha = 0.01$.

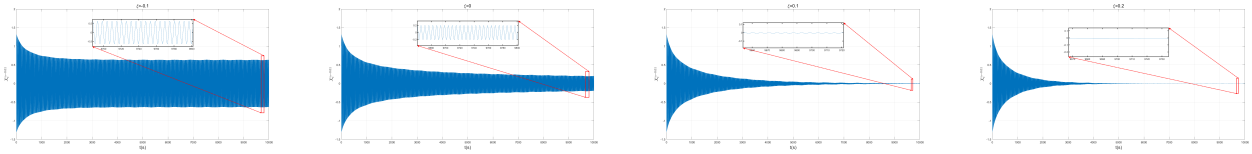

**(a)** $\xi = -0.1$ **(b)** $\xi = 0$ **(c)** $\xi = 0.1$ **(d)** $\xi = 0.2$

**Figure 4.** The 2D plot of the $\alpha$-path for the parameter values $\xi = [-0.1, 0, 0.1, 0.2]$ at $\alpha = 0.45$.

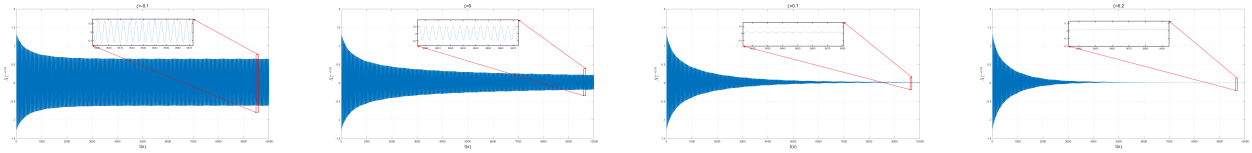

**(a)** $\xi = -0.1$ **(b)** $\xi = 0$ **(c)** $\xi = 0.1$ **(d)** $\xi = 0.2$

**Figure 5.** The 2D plot of the $\alpha$-path for the parameter values $\xi = [-0.1, 0, 0.1, 0.2]$ at $\alpha = 0.99$.

Figure 6 illustrates the periodic results computed using the spectral method based on Eq (4.1). The left column displays the variations of errors with respect to the event sequence, while the right column corresponds to the power spectral density of the left images, with the unique peak value indicating the period.

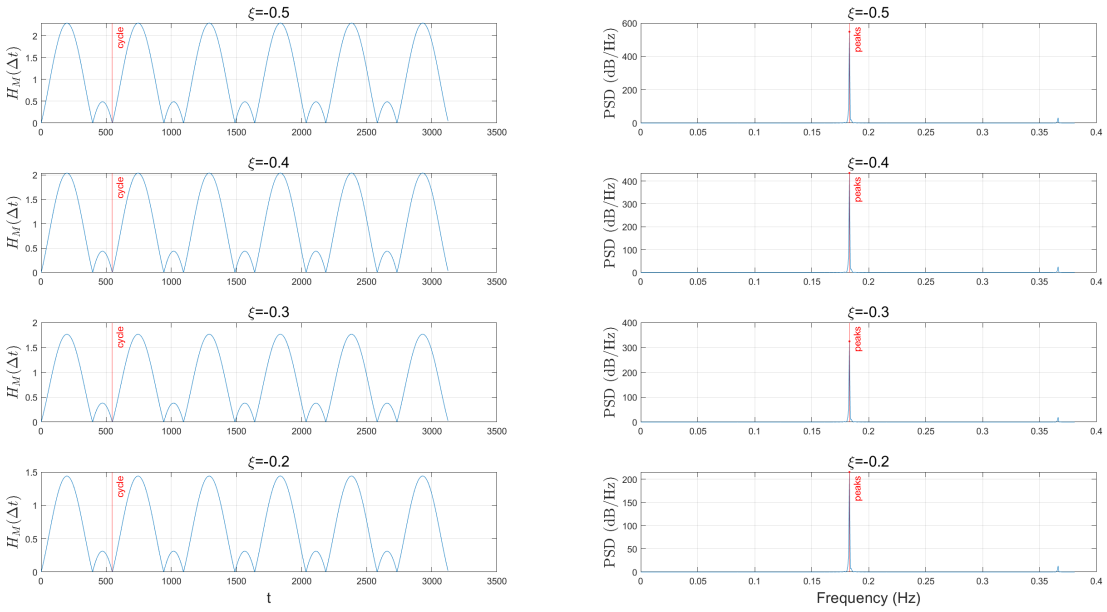


**Figure 6.** The period of $\alpha$-path for the parameter values $\xi = [-0.5, -0.4, -0.3, -0.2]$ .

Figure 7 demonstrates that the uncertainty distribution at intervals of one period is nearly identical,

while the distribution at intervals of $T/2$ exhibits significant differences. This observation provides evidence for the periodic characteristics of the uncertainty distribution.

**Remark 4.1.** *In fact, in Figure 7, the inverse distribution of uncertain variables at moments like $T/3, T/4$ could be taken. Considering the differences are most evident at the $T/2$ moment, the inverse distribution at the $T/2$ moment was chosen for comparison.*

The results in Figure 8 demonstrate a substantial overlap among the three, confirming the stability of the uncertainty distribution.

2) $\gamma < 0$: In Figure 9, zone 1 exhibits divergence, zone 3 represents asymptotically stable behavior, and zone 2 signifies the transitional zone. In theory, zone 1 should be infinite; however, for the purpose of numerical simulation, it is truncated to 100, resulting in a logarithmic value of 2. When $\gamma < 0$, the characteristic variation of the $\alpha$-path resembles a subcritical Hopf bifurcation, accompanied by the gradual disappearance of an unstable limit cycle. The $\alpha$-path demonstrates a transition from divergence to asymptotic stability, and due to the clear transition from divergence to asymptotic stability, the boundary between the unstable and stable zones is also distinct. Similarly, the attraction basin in Figure 10 also confirms the existence of unstable limit cycles.

In Figure 11, the $\alpha$-path under parameter $\xi = [-0.1, 0, 0.1, 0.2]$ reveals a transition from divergence to stability in the amplitude.

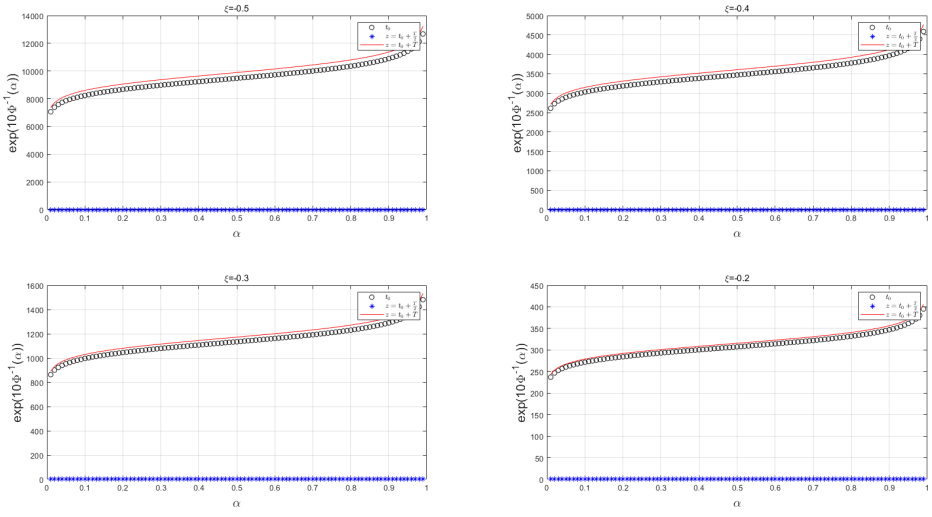


**Figure 7.** Inverse distribution plot. The inverse distribution at $t_0, t_0 + T/2, t_0 + T$ moments of uncertainty were plotted for the periodic solutions corresponding to Figure 1 Zeon1, which were obtained using Eq (4.1) for bifurcation points$(-0.5, -0.4, -0.3, -0.2)$.This figure is computed from Eq (3.9b), where $T \approx 5.46$ s.

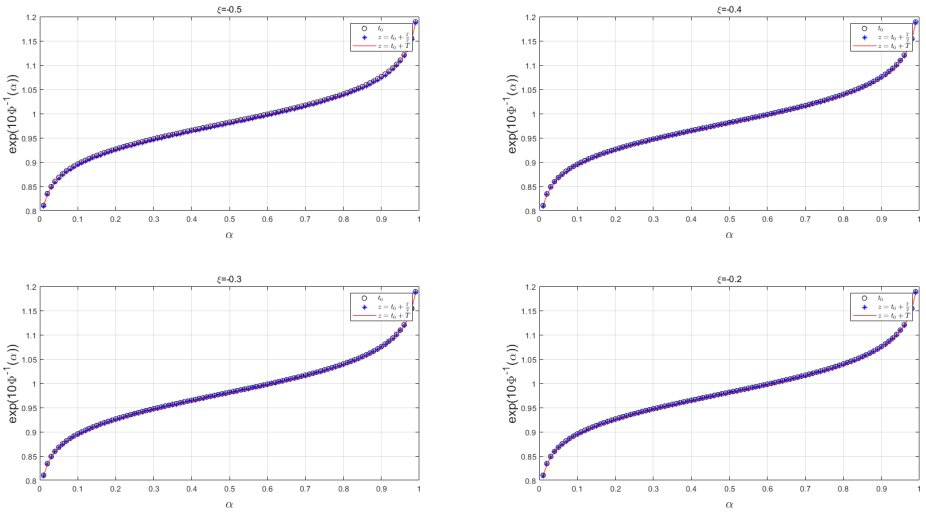


**Figure 8.** Inverse distribution plot. In the case of bifurcations at $(0.5, 0.4, 0.3, 0.2)$, this section corresponds to asymptotic stability, as depicted in Figure 1 Zeon3. Similarly, inverse uncertainty distribution plots were generated at moments $t_0, t_0 + T/2, t_0 + T$. This figure is computed from Eq (3.9b), where $T \approx 5.46$s.

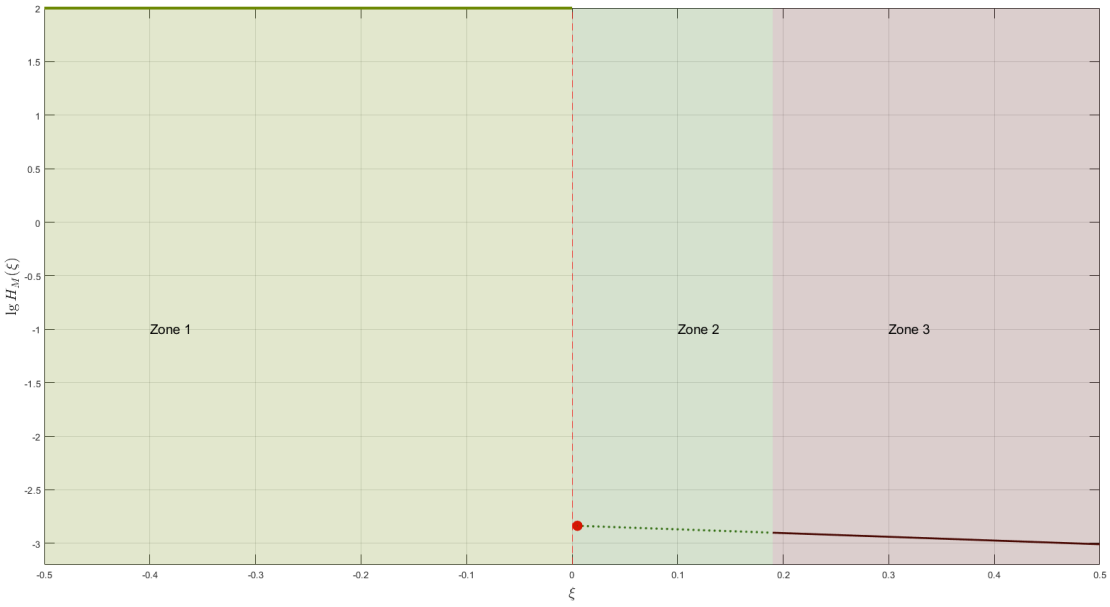


**Figure 9.** Bifurcation diagram. This figure is computed from Eq (3.9b), where $\Delta t = 0.01; n = 2 \times 10^6$.

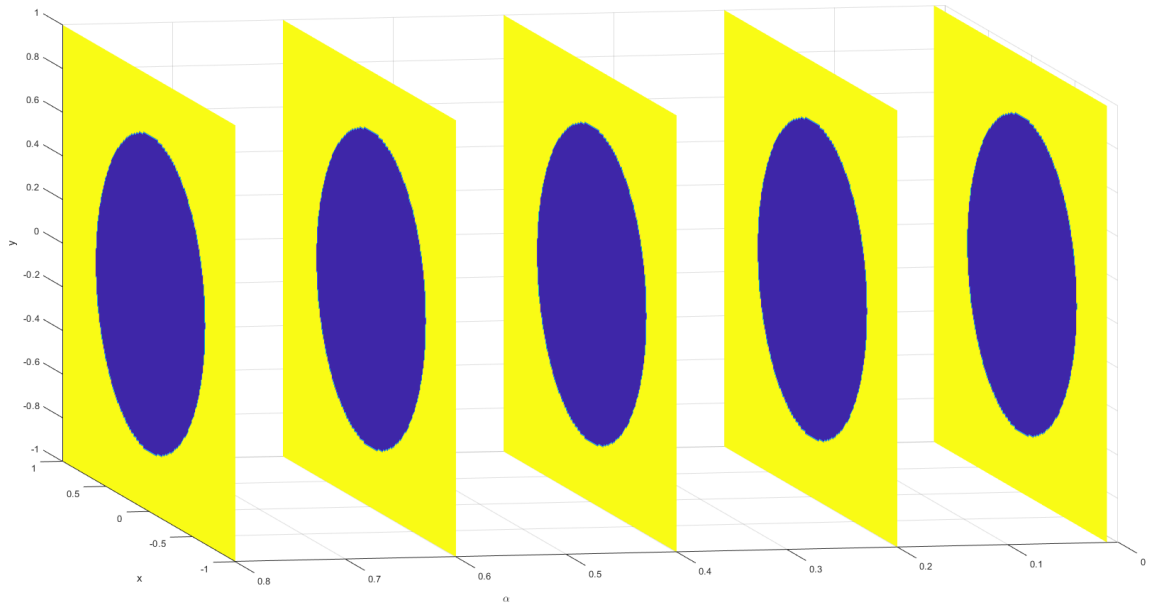

**Figure 10.** Attracting basin. The blue zone represents the basin of attraction around the origin, while the yellow zone represents the basin of attraction extending to infinity, and the boundary between the yellow and blue zones depicts an unstable limit cycle.

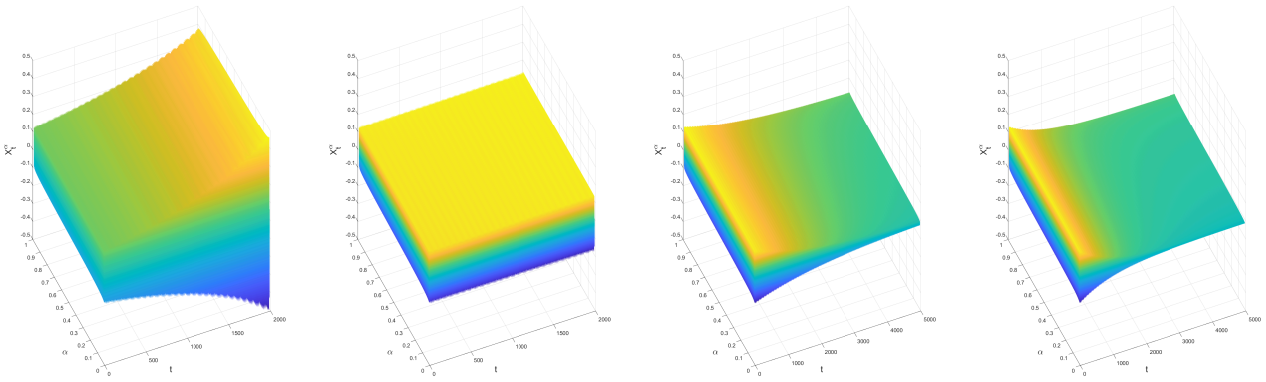

**(a)** $\xi = -0.1$ **(b)** $\xi = 0$ **(c)** $\xi = 0.1$ **(d)** $\xi = 0.2$

**Figure 11.** The three-dimensional plot of the $\alpha - path$. The three-dimensional plot of the $\alpha$-path under the parameter $\xi = [-0.1, 0, 0.1, 0.2]$. The plot reveals a consistent trend in all $\alpha - path$ as $\xi$ increases: a transition from divergence to asymptotic stability.

Figures 12 ($\alpha$=0.01), 13 ($\alpha$=0.45), and 14 ($\alpha$=0.99) display different $\alpha$-paths, with their two-dimensional trajectories providing important findings that complement the three-dimensional representation in Figure 12. Collectively, they reveal the following pattern: although all $\alpha$-paths undergo a unified bifurcation behavior transitioning from unstable periodicity to asymptotic stability

near $\xi$=0.1, indicating that $\xi$ is the key parameter controlling the stability transition of the system, the value of $\alpha$ significantly influences the convergence characteristics after bifurcation. As $\alpha$ increases from 0.01 to 0.99, the system demonstrates a clear progression from slow decay with persistent oscillations to rapid stabilization.

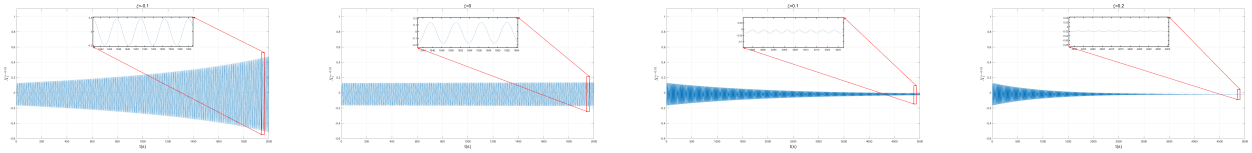

**(a)** $\xi = -0.1$ **(b)** $\xi = 0$ **(c)** $\xi = 0.1$ **(d)** $\xi = 0.2$

**Figure 12.** The 2D plot of the $\alpha$-path for the parameter values $\xi = [-0.1, 0, 0.1, 0.2]$ at $\alpha = 0.01$.

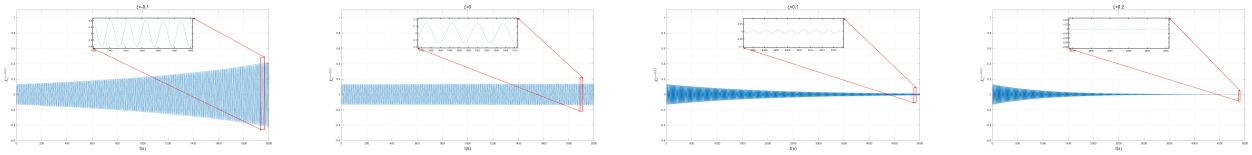

**(a)** $\xi = -0.1$ **(b)** $\xi = 0$ **(c)** $\xi = 0.1$ **(d)** $\xi = 0.2$

**Figure 13.** The 2D plot of the $\alpha$-path for the parameter values $\xi = [-0.1, 0, 0.1, 0.2]$ at $\alpha = 0.45$.

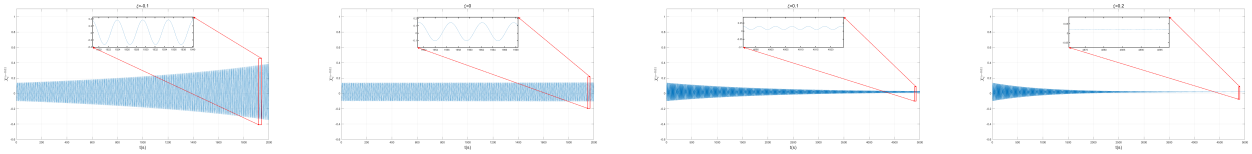

**(a)** $\xi = -0.1$ **(b)** $\xi = 0$ **(c)** $\xi = 0.1$ **(d)** $\xi = 0.2$

**Figure 14.** The 2D plot of the $\alpha$-path for the parameter values $\xi = [-0.1, 0, 0.1, 0.2]$ at $\alpha = 0.99$.

## 5. Conclusions

This study extends the classical Hopf bifurcation theory of deterministic differential equations to UDEs by utilizing the cross-entropy of the inverse distribution, where the inverse distribution is determined through the $\alpha$-path. The paper designs an efficient algorithm to verify the uncertain Hopf bifurcation and quantify the bifurcation threshold, and the validity of the defined uncertain Hopf bifurcation is confirmed through numerical simulations. The paper also proposes an improved fourth-order Runge-Kutta method to solve high-order UDEs, and the effectiveness and efficiency of this method are demonstrated through numerical experiments.

This paper initiates the study of Hopf bifurcation in UDEs, representing an effective integration of uncertain theory with nonlinear dynamics theory, thereby expanding the application of uncertain

theory. At the same time, it provides a method for studying dynamic transition problems involving frequency instability in practical engineering. Building on the research presented in this paper, we will also delve into the chaos theory of uncertain systems in the future, such as extending chaos criteria like the Lyapunov method and the Melnikov method to higher-order UDEs.

## Author contributions

Xiuying Guo: Writing—original draft, methodology; Caiyun Huang: Writing—original draft, writing—review and editing; Qiubao Wang: Methodology; Zikun Han: Writing—review and editing, software; Zeman Wang: Writing—original draft; Xiyuan Chen: Software. All authors have read and agreed to the published version of the manuscript.

## Use of Generative-AI tools declaration

The authors declare that they have not used Artificial Intelligence (AI) tools in the creation of this article.

## Acknowledgments

This work was supported by National Natural Science Foundation of China [No.U23A2068]; Top-notch Young Talent Program of Hebei Province Education Department of China (BJK2023037).

## Conflict of interest

The authors declare no conflicts of interest.

## References

1. I. M. Elbaz, M. A. Sohaly, H. El-Metwally, Random dynamics of an SIV epidemic model, *Commun. Nonlinear Sci. Numer. Simul.*, **131** (2024), 107779. https://doi.org/10.1016/j.cnsns.2023.107779
2. R. Ceccon, G. Livieri, S. Marmi, The Yoccoz Birkeland livestock population model coupled with random price dynamics, *Commun. Nonlinear Sci. Numer. Simul.*, **118** (2023), 106982. https://doi.org/10.1016/j.cnsns.2022.106982
3. C. Fan, J. Wu, T. Yao, H. Xiao, J. Xu, J. Leng, et al., Investigation of pump scheme on the dynamics of brightness-enhanced random Raman fiber lasers, *Opt. Laser Technol.*, **172** (2024), 110507. https://doi.org/10.1016/j.optlastec.2023.110507
4. J. Lin, P. B. Kahn, Random effects in population models with hereditary effects, *J. Math. Biol.*, **10** (1980), 101–112. https://doi.org/10.1007/BF00275836
5. D. Kahneman, A. Tversky, Prospect theory: An analysis of decisions under risk, *Econometrica*, **47** (1979), 263–291. https://doi.org/10.1017/CBO9780511609220.014
6. B. Liu, *Uncertainty theory*, 4 Eds., Berlin, Heidelberg: Springer, 2015. https://doi.org/10.1007/978-3-662-44354-5

7. J. B. Walsh, An introduction to stochastic partial differential equations, In: *École d'Été de Probabilités de Saint Flour XIV - 1984*, **1180** (1986), 265–439. https://doi.org/10.1007/BFb0074920
8. P. L. Chow, Generalized solution of some parabolic equations with a random drift, *Appl. Math. Optim.*, **20** (1989), 1–17. https://doi.org/10.1007/bf01447642
9. K. Peter, Existence, uniqueness and smoothness for a class of function valued stochastic partial differential equations, *Stoch. Stoch. Rep.*, **41** (1992), 177–199. https://doi.org/10.1080/17442509208833801
10. S. Peszat, J. Zabczyk, Stochastic evolution equations with a spatially homogeneous Wiener process, *Stoch. Proc. Appl.*, **72** (1997), 187–204. https://doi.org/10.1016/s0304-4149(97)00089-6
11. X. Yang, K. Yao, Uncertain partial differential equation with application to heat conduction, *Fuzzy Optim. Decis. Making*, **16** (2017), 379–403. https://doi.org/10.1007/s10700-016-9253-9
12. Z. Peng, K. Iwamura, A sufficient and necessary condition of uncertainty distribution, *J. Interdiscip. Math.*, **13** (2010), 277–285. https://doi.org/10.1080/09720502.2010.10700701
13. B. Liu, Some research problems in uncertainty theory, *J. Uncertain Syst.*, **3** (2009), 3–10.
14. B. Liu, Uncertain reliability analysis, In: *Uncertainty theory: A Branch of mathematics for modeling human uncertainty*, **300** (2010), 125–130. https://doi.org/10.1007/978-3-642-13959-8_4
15. B. Liu, Fuzzy process, hybrid process and uncertain process, *J. Uncertain Syst.*, **2** (2008), 3–16.
16. X. Chen, B. Liu, Existence and uniqueness theorem for uncertain differential equations, *Fuzzy Optim. Decis. Making*, **9** (2010), 69–81. https://doi.org/10.1007/s10700-010-9073-2
17. K. Yao, J. Gao, Y. Gao, Some stability theorems of uncertain differential equation, *Fuzzy Optim. Decis. Making*, **12** (2013), 3–13. https://doi.org/10.1007/s10700-012-9139-4
18. K. Yao, A type of uncertain differential equations with analytic solution, *J. Uncertain. Anal. Appl.*, **1** (2013), 8. https://doi.org/10.1186/2195-5468-1-8
19. Y. Liu, An analytic method for solving uncertain differential equations, *J. Uncertain Syst.*, **6** (2012), 244–249.
20. Y. Sheng, J. Gao, Exponential stability of uncertain differential equation, *Soft Comput.*, **20** (2016), 3673–3678. https://doi.org/10.1007/s00500-015-1727-0
21. K. Yao, H. Ke, Y. Sheng, Stability in mean for uncertain differential equation, *Fuzzy Optim. Decis. Making*, **14** (2015), 365–379. https://doi.org/10.1007/s10700-014-9204-2
22. L. Yang, Y. Liu, Solution method and parameter estimation of uncertain partial diferential equation with application to China's population, *Fuzzy Optim. Decis. Making*, **23** (2024), 155–177. https://doi.org/10.1007/s10700-023-09415-5
23. Y. Liu, B. Liu, Estimating unknown parameters in uncertain differential equation by maximum likelihood estimation, *Soft Comput.*, **26** (2022), 2773–2780. https://doi.org/10.1007/s00500-022-06766-w
24. Z. M. Wang, Z. Liu, Z. K. Han, X. Y. Guo, Q. B. Wang, The inverse uncertainty distribution of the solutions to a class of higher-order uncertain differential equations, *AIMS Mathematics*, **9** (2024), 33023–33061. https://doi.org/10.3934/math.20241579

25. K. Yao, X. Chen, A numerical method for solving uncertain differential equations, *J. Intell. Fuzzy Syst.*, **25** (2013), 825–832. https://doi.org/10.3233/ifs-120688
26. K. Yao, Extreme values and integral of solution of uncertain differential equation, *J. Uncertain. Anal. Appl.*, **1** (2013), 2. https://doi.org/10.1186/2195-5468-1-2
27. X. Yang, Y. Shen, Runge-Kutta method for solving uncertain differential equations, *J. Uncertain. Anal. Appl.*, **3** (2015), 17. https://doi.org/10.1186/s40467-015-0038-4
28. X. Yang, D. A. Ralescu, Adams method for solving uncertain differential equations, *Appl. Math. Comput.*, **270** (2015), 993–1003. https://doi.org/10.1016/j.amc.2015.08.109
29. X. Wang, Y. Ning, T. A. Moughal, X. Chen, Adams Simpson method for solving uncertain differential equation, *Appl. Math. Comput.*, **271** (2015), 209–219. https://doi.org/10.1016/j.amc.2015.09.009
30. R. Gao, Milne method for solving uncertain differential equations, *Appl. Math. Comput.*, **274** (2016), 774–785. https://doi.org/10.1016/j.amc.2015.11.043
31. K. Yao, *Uncertain differential equations*, Berlin, Heidelberg: Springer, 2016. https://doi.org/10.1007/978-3-662-52729-0
32. Y. Hou, L. Wu, Y. Sheng, Solving high-order uncertain differential equations via Adams–Simpson method, *Comput. Appl. Math.*, **40** (2021), 252. https://doi.org/10.1007/s40314-020-01408-z
33. X. Ji, J. Zhou, Solving high-order uncertain differential equations via Runge–Kutta method, *IEEE Trans. Fuzzy Syst.*, **26** (2017), 1379–1386. https://doi.org/10.1109/tfuzz.2017.2723350
34. J. Kuang, M. Wang, J. Han, Y. Sheng, Improved Milne-Hamming method for resolving high-order uncertain differential equations, *Appl. Math. Comput.*, **457** (2023), 128199. https://doi.org/10.1016/j.amc.2023.128199
35. J. E. Marsden, M. McCracken, *The Hopf bifurcation and its applications*, New York: Springer, 1976. https://doi.org/10.1007/978-1-4612-6374-6
36. G. Iooss, *Bifurcation of maps and applications*, Elsevier, 1979.
37. S. Wiggins, *Introduction to applied nonlinear dynamical systems and chaos*, New York: Springer, 2003. https://doi.org/10.1007/b97481
38. X. F. Liao, G. R. Chen, Hopf bifurcation and chaos analysis of Chen's system with distributed delays, *Chaos Soliton Fract.*, **25** (2005), 197–220. https://doi.org/10.1016/j.chaos.2004.11.007
39. Q. B. Wang, Z. K. Han, X. Zhang, Y. J. Yang, Dynamics of the delay-coupled bubble system combined with the stochastic term, *Chaos Soliton Fract.*, **148** (2021), 111053. https://doi.org/10.1016/j.chaos.2021.111053
40. W. Q. Zhu, Z. L. Huang, Stochastic Hopf bifurcation of quasi-nonintegrable-Hamiltonian systems, *Int. J. Non-Linear Mech.*, **34** (1999), 437–447. https://doi.org/10.1016/S0020-7462(98)00026-2
41. X. Gao, L. F. Jia, S. Kar, A new definition of cross-entropy for uncertain variables, *Soft Comput.*, **22** (2018), 5617–5623. https://doi.org/10.1007/s00500-017-2534-6


AIMS Press